Fabrication of 3-diethylaminopropylamine modified bamboo fiber prepared by radiation technique and its efficient and recycle adsorption for methyl orange

Houhua Xiong[a], Zhengkui Zeng[a],*, Jifu Du[a], Long Zhao[b],*

[a]School of Nuclear Technology and Chemistry & Biology, Hubei University of Science and Technology, Xianning 437100, emails: zengzk@hbust.edu.cn (Z. Zeng), xionghouhua@hbust.edu.cn (H. Xiong), duzidedu@163.com (J. Du)
[b]State Key Laboratory of Advanced Electromagnetic Engineering and Technology, School of Electrical and Electronic Engineering, Huazhong University of Science and Technology, Wuhan 430074, China, email: zhaolong@hust.edu.cn/ ryuuchou@hotmail.com (L. Zhao)

ABSTRACT

The excessive discharge of dye wastewater present certain hazards to human health and the environment. The removal of dyes from the aquatic environment is vital necessary. In this paper, a quaternized bamboo fiber (QBF) was successfully prepared by radiation induced graft-polymerization and further modification. The QBF was characterized by thermogravimetric, infrared and scanning electron microscopy analyses. The adsorption of methyl orange dye (MO) by the QBF was studied under different conditions. The adsorption kinetic study indicated that the adsorption was followed by pseudo-second-order model and the saturation equilibrium was reached in 60 min. The adsorption isotherm was well obeyed the Langmuir model with a maximum theoretical adsorption capacity of 555.56 mg/g. The QBF can be effectively desorbed by 1 M HCl and reused. Therefore, the QBF prepared using the radiation technique can be potentially applied to the removal of MO dye in wastewater.

Keywords: Bamboo fiber; Methyl orange; Adsorption; Radiation technique

1. Introduction

With the continuous development of printing, leather, textiles, paper, plastics, and rubber industries, dye pollutants have become one of the main sources of water pollution. The discharge of dye wastewater from various industries is a great threat to the human body and the environment. Azo dyes, characterized by an azo bond (–N=N–), constitute 60%–70% of organic dyes [1,2]. Methyl orange (MO), a typical azo dye, is not only used as an acid–base indicator for chemical products in industrial and agricultural production, but also used as a dye in the printing and dyeing industry. Due to the distinct color of azo dye wastewater, it can adversely affect the photosynthesis of plants in the ecological environment. Furthermore, when water source are

contaminated, the associated low toxicity will also accumulate in human society, and causing potential harm [3].

Currently, numerous methods are known for treating dye wastewater, including membrane filtration [4], electrochemical oxidation [5,6], biological treatment [7], coagulation [8], and degradation etc. [9,10]. However, most of the above methods come with several drawbacks such as complexity, high energy costs, time-consuming, and the formation of by-products [11]. In contrast, adsorption offers advantages such as simple design and operation, high removal efficiency, low operational cost, and no pollution, making it particularly suitable for treating low concentration wastewater [12,13].

Various adsorbents including activated carbon, biochar, polymers and resins, clays and minerals, bio-adsorbent,

* Corresponding authors.

nanoparticles are employed for MO adsorption [14–18]. Especially, low-cost biomass are being considered as promising adsorbents because of the low-cost, reusable and biodegradable [19]. Bamboo cellulose, derived from an abundant and renewable resource, possesses numerous advantages such as low cost, natural biodegradable, and loose structure. In recent years, bamboo has been converted to activated carbon or bamboo charcoal, which is recognized as one of the most lucrative adsorbents [20–22].

However, the chemical structure makes bamboo low reactivity, with fewer functional groups, resulting in a weak adsorption capacity for natural cellulose. This limitation restricts its application in the adsorption field. Therefore, addressing the enrichment of functional groups of bamboo becomes a matter of deep concern, crucial for providing bamboo with promising prospect in environmental fields [23].

Dual functional monomer like 3-diethylaminopropylamine monomer (DEAPA) are attractive due to their combination of an epoxy reactive primary amine and a positively charged tertiary amine [24]. The primary amine can easily undergo ring opening with epoxy groups. For this reason, DEAPA can easily immobilized on epoxy group modified substrate, thus make tertiary amine becomes a functional group fixed on the surface of the substrate [25,26]. The tertiary amine grafted material has been demonstrated to exhibit a strong affinity towards dye molecules [27].

Glycidyl methacrylate is a commercially available vinyl monomer which contains an oxirane group. In our previous study, cellulose modified with glycidyl methacrylate (GMA) was prepared using the electron beam radiation technique, and followed by additional modification. The modification endowed the cellulose substrate with a specific adsorption ability for heavy metals [28], gold ions [29], phosphate [30], radioactive nuclei [31,32], semi-metals [33], and dyes [34]. Compared to traditional chemical modification methods, radiation induced graft polymerization provides an attractive approach for modifying the physicochemical properties of polymer materials. Radiation induced graft polymerization has numerous advantages including being relatively easier to operate, more environmentally friendly, operating at room temperature, requiring no poisonous chemicals, and high grafting rate [35–37].

In this paper, bamboo fiber grafted with GMA through radiation induced graft polymerization was employed as a substrate. Following the ring-opening reaction with DEAPA and subsequent quaternization reaction, the resulting quaternized bamboo fiber (QBF) was prepared. It is expected to remove methyl orange (MO) quickly and effectively from aqueous solution.

2. Experimental set-up

2.1. Materials

Bamboo was collected from *Phyllostachys pubescens* (Xianning City, Hubei, China), then split into very thin strips. The bamboo fiber (BF) was obtained after treating the bamboo strips at 100°C in a 1 M NaOH solution for 1 h. GMA, Tween 20, DEAPA, iodomethane, and methyl orange (MO) were supplied by Macklin Chemical Reagent Limited Corporation (China). The molecular structure of MO is shown in Fig. 1.

2.2. Preparation of QBF

The QBF were synthesized using the electron beam radiation induced grafting technique, and the synthesis route is illustrated in Fig. 2. The procedure was similar to that reported by the study of Du et al. [38,39]. Firstly, the GMA emulsion aqueous solution contains 30 wt.% GMA and the emulsifying agent (3 wt.% tween 20) was bubbled with N_2 for 30 min to remove oxygen. The dry BFs (2 g) was pouched into a vacuum sealed polyethylene bags. GMA emulsion with 30 mL was injected into the bags using a syringe. The bags were irradiated by electron beam under the accelerator (Wasik Associates INC, USA) at 1 MeV. The irradiation delivered a dose of 10 kGy/pass and the total dose of 60 kGy. After irradiation, the GMA grafted BF (BF-GMA) was obtained after washing and drying. The mass increase ratio before and after grafting was 265.6 wt.%.

Secondly, 0.5 g BF-GMA was immersed in a 50 mL aqueous solution containing 15 mL DEAPA. Then the reaction maintained 6 h at 80°C. After reaction, the excess unreacted DEAPA was removed by pure water to obtain BF-GMA-DEAPA. The mass increase ratio before and after reaction is 24 wt.%.

Finally, the BF-GMA-DEAPA was quaternized in a solution (3 mL iodomethane and 47 mL H_2O) for 24 h at 30°C and kept in a dark place. After washing and drying to a constant weight, the QBF was obtained.

2.3. Characterization

Thermogravimetric (TG) analysis was employed to test the thermal stability using a TG290F3 Instrument of Netzsch
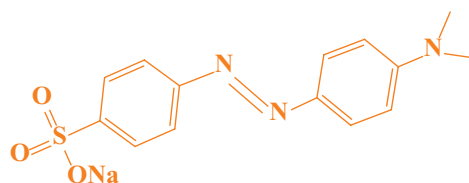
Fig. 1. Molecular structure of methyl orange.
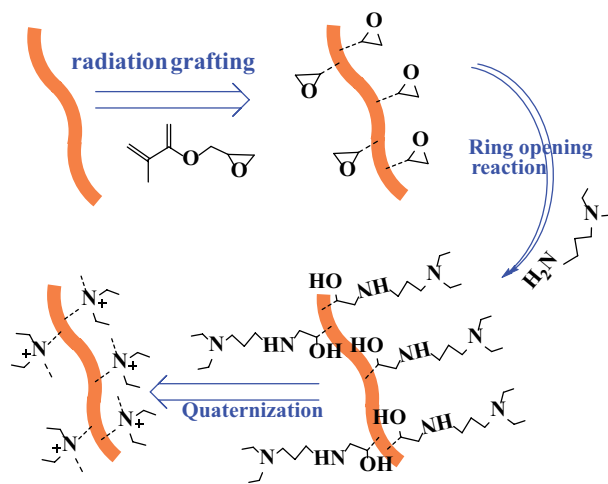
Fig. 2. Preparation route of quaternized bamboo fiber.

at the temperature from 20°C to 600°C under N$_2$ atmosphere. Fourier-transform infrared spectroscopy (FTIR) spectra were analyzed on Spectrum Two (PerkinElmer, USA) with the wavenumber range 4,000–400 cm^{-1}. Scanning electron microscopy (SEM; TESCAN Vega3, Czech) was used to observe the surface morphologies of materials. Zeta potential was measured with a 90Plus PALS system (Brookhaven Instruments Corp., USA).

2.4. Analysis of dye concentration in test solution

The concentrations of MO were measured using a UV-Vis spectrophotometer (UV-1800PC, Aoyi Instruments (Shanghai) Co., Ltd., China) at the wavelength of 468 nm.

2.5. Batch adsorption experiments

The investigation of different factors such as pH, contact time, dosage, and initial concentration on adsorption capacity was conducted following a very similar procedure. For the pH effect study, QBF with a mass of 0.05 g was put into 50 mL, 50 mg/L MO aqueous solution, and shaken at 120 rpm at 25°C for 24 h. After adsorption, the supernatant was filtered with a 0.45 μm filter. In the studies of different adsorption time (*t*) and isotherm studies, a mass 0.03 g was utilized. For isotherm studies, the initial MO concentration were varied from 100 to 1,000 mg/L to achieve equilibrium adsorption. In the ionic strength study, the molar ratio of NaCl/MO varified from 1:1 to 1:1,000. The adsorption capacity (Q_t) and removal efficiency of MO onto the QBF were calculated using Eqs. (1) and (2):

$$Q_t = \frac{(C_0 - C_t)V}{m} \tag{1}$$

$$\text{Removal \%} = \frac{C_0 - C_t}{C_0} \times 100 \tag{2}$$

where C_0 and C_t represent the concentration before and after adsorption. *V* (L) represents the volume and *m* (g) was the QBF weight. The experiments was conducted parallel sample and the averaging was used.

3. Results and discussion

3.1. Characterization

FTIR analysis was carried out to verify the grafting and modification of BF by DEAPA, which is depicted in Fig. 3a. For BF, the bands at 2,898 and 1,050 cm^{-1} were attributed to C–H and C–O bonding, respectively. After GMA grafted, two sharp bands at 1,729 and 909 cm^{-1} assigned to C=O band and epoxy group of GMA appeared, confirming the successful grafting of GMA on BF [29,30,40]. After ring-opening reaction, the bands at 1,571 cm^{-1} was corresponded to the N–H band of DEAPA [41]. In the QBF sample, the band at 1,640 cm^{-1}, the characteristic band of quaternary nitrogen appeared, indicated the tertiary amine of was converted into the quaternary ammonium group [42,43].

Fig. 3b shows the TG curves of BF and DEAPA modified BF. BF showed a high decomposition temperature beyond 300°C with a one-step weight loss. BF-GMA began to decompose at 300°C. BF-GMA-DEAPA and QBF began to decompose at 250°C, showing multiple loss zones. The results showed that the thermal stability of BF decreased after modification, however, it remains adequate for use in water environmental disposal.

Fig. 4 shows the SEM micromorphology of BF and modified BF. The surface images of BF depicted an order and smooth fiber. After GMA grafted and DEAPA modification, the surface became rougher, confirming the successful chemical modification of the BF.

3.2. Batch adsorption experiment

3.2.1. pH effect and zeta potential

The solution pH significantly influenced adsorption process, as pH can affect the surface charge of both the adsorbate and adsorbent. The adsorption capacity of MO by QBF at different pH is shown in Fig. 5a. Below pH 4, the adsorption capacity is lower, and increases at pH 4, then remains unchanged between pH 4 to 11. Fig. 5b shows the zeta potential (mV) of QBF, with positive values observed across all pH range. However, these values are lower under acidic conditions and higher at pH > 4. The zeta potential value exhibit a similar trend with the adsorption results at different pH
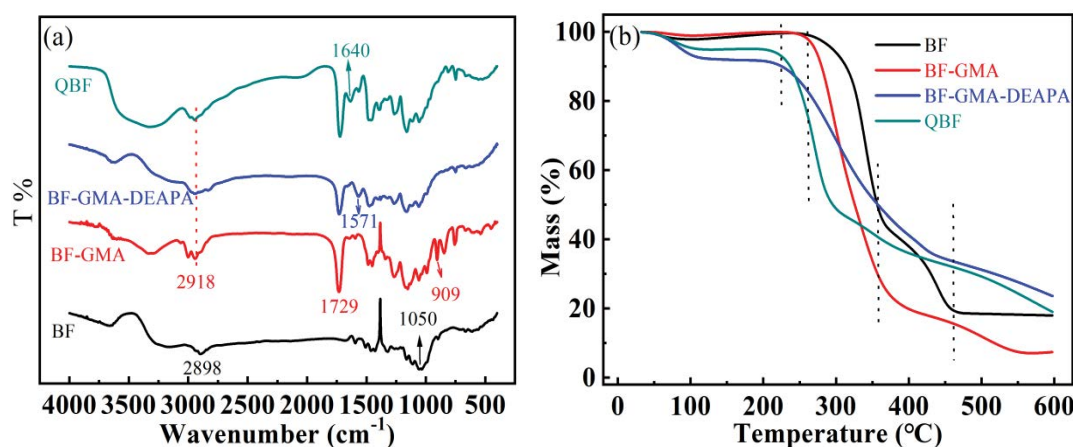
Fig. 3. Fourier-transform infrared spectroscopy (a) and thermogravimetric curves (b) of BF and DEAPA modified BF.
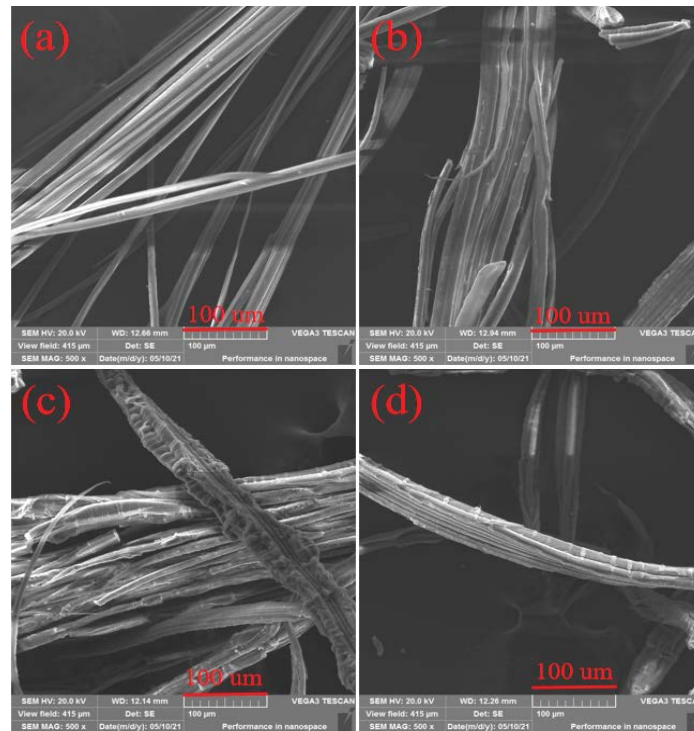
Fig. 4. Scanning electron micromorphology of BF (a), BF-GMA (b), BF-GMA-DEAPA (c) and quaternized bamboo fiber (d).
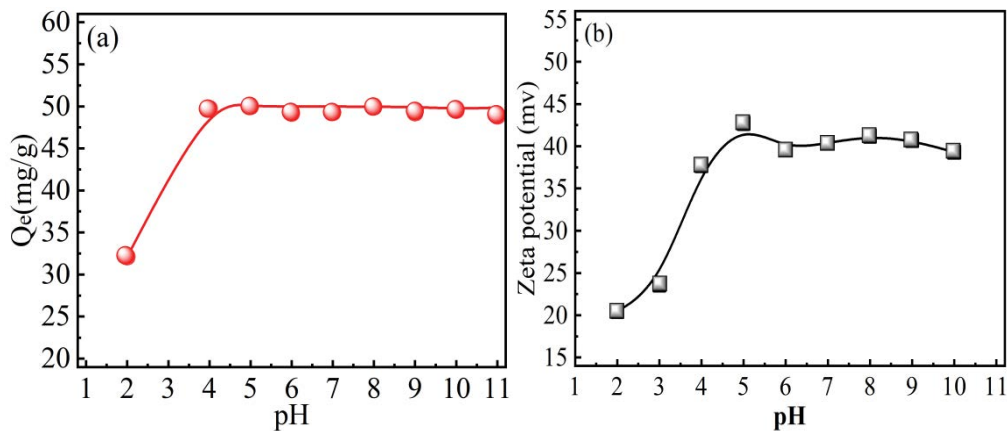
Fig. 5. Effect of pH for methyl orange adsorption (a) and zeta potential of quaternized bamboo fiber (b).

value. Given that the dissociation constant (pKa) of MO was 3.46, the positive charge will generated at higher pH values results in a strong electrostatic attraction to negative MO molecule, especially at pH above 3.46. Based on the results, at pH > 4, the electrostatic attraction between –N$^+$(C$_2$H$_5$)$_2$CH$_3$ on QBF and –SO$_3^-$ is enhanced. Therefore, in further exploration experiments, we conducted the experiments at natural pH of about 5 without adjusting the pH.

3.2.2. Effect of dosage

The adsorption performance for MO was investigated with different mass of QBF. The relationship between the adsorption capacity/removal efficiency and the dosage at pH

5 is shown in Fig. 6. The adsorption capacity of MO reached 235.57 mg/g with a mass of 0.01 g, and decreased with the mass increasing. The removal efficiency increased sharply from a mass of 0.01 to 0.03, attributed to more functional groups working for MO adsorption. With a mass >0.03 g, the removal efficiency remained above 99%. In this work, a dosage (0.03 g QBF in 50 mL MO) was used for further adsorption experiments.

3.2.3. Adsorption kinetics: effect of contact time

The adsorption kinetics are of great significance for determining the adsorption mechanisms. Fig. 7a shows the influence of the contact time on the adsorption capacity of

MO. The adsorption gradually increased with the contact time and finally reached a maximum value at 60 min and then remaining constant value.

There are several kinetic models used to analysis the adsorption and diffusion process. In this study, the experimental data were fitted by pseudo-first-order, pseudo-second-order and intraparticle diffusion model, which were described by Eqs. (3)–(5), respectively [44].

$$\ln\left(Q_e - Q_t\right) = \ln Q_e - k_1 t \tag{3}$$

$$\frac{t}{Q_t} = \frac{1}{k_2 Q_e^2} + \frac{t}{Q_e} \tag{4}$$

$$Q_t = k_{in} t^{1/2} + I \tag{5}$$

where Q_t and Q_e are the amounts of MO adsorbed on 1 g QBF at time t and the equilibrium time, respectively.

The linear fitting curves of the three models are shown in Fig. 7b–d. The results showed that the adsorption kinetics could be well fitted by both pseudo-first-order and pseudo-second-order models, implying that the adsorption of MO involving both physical and chemical adsorption. The linear fitted plot of the intraparticle diffusion model shows three linear regions. According to the model, the first linear part represents the transport of MO molecular from the solution to the QBF surface, the second region represents the gradual adsorption corresponding to intraparticle diffusion, and the third part indicates the equilibrium
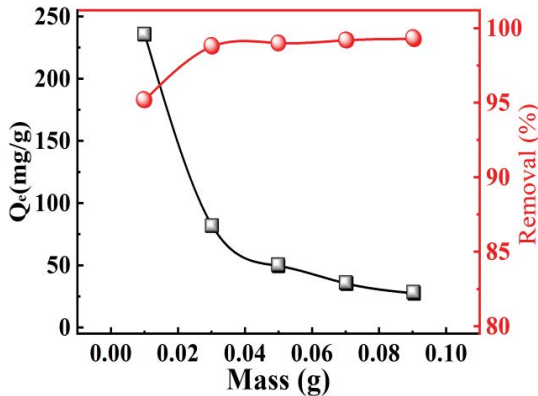
Fig. 6. Effect of dosage on the adsorption (pH 5; C_0 = 50 mg/L; V = 50 mL).
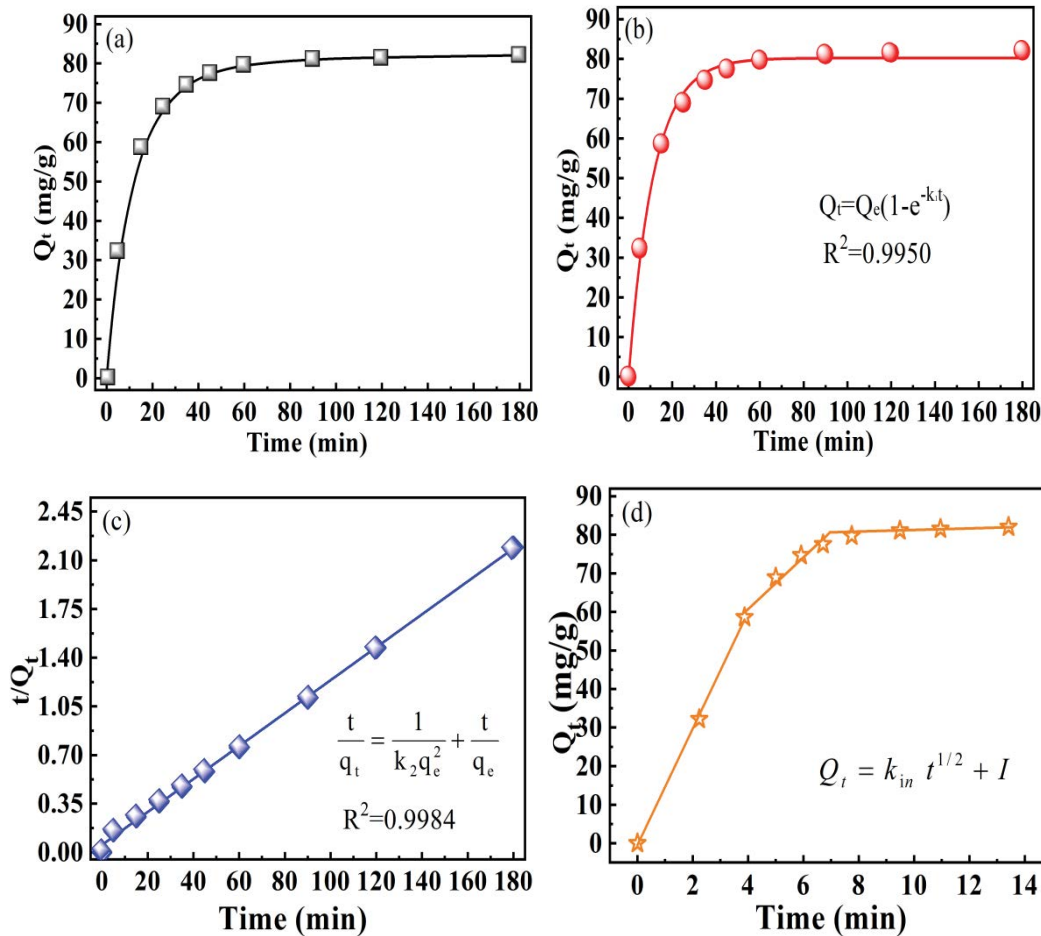
Fig. 7. Influence of the contact time on the adsorption capacities (a), pseudo-first-order (b), pseudo-second-order (c) and intraparticle model (d).

has been attained. The first linear plot nearly passed through the origin, indicating that the adsorption rate of MO by QBF were primarily controlled by intraparticle diffusion models.

3.2.4. Adsorption isotherm

The adsorption isotherm is used to describe the distribution of target ions on the adsorbent surface and calculate the maximum adsorption capacity (Q_e). Fig. 8a shows the relationship between the adsorption capacity and equilibrium concentration. The adsorption capacity increases with the initial concentration. Two isotherm models, Langmuir and Freundlich are applied to fit the adsorption isotherm, which linear forms can be described by Eqs. (6) and (7) [45].

$$\frac{C_e}{Q_e} = \frac{C_e}{Q_m} + \frac{1}{K_L Q_m} \tag{6}$$

$$\ln Q_e = \ln K_F + \frac{1}{n} \ln C_e \tag{7}$$

where C_e is the equilibrium concentration (mg/L), Q_e (mg/g) presents the mass of MO adsorbed on 1 g QBF (mg/g).

Fig. 8b and c show the fitting Langmuir and Freundlich curves, which fitting parameters is listed in Table 2. Langmuir model has a higher R^2 value, suggesting that MO formed a monolayer on the surface of QBF [46]. The calculated

maximum adsorption capacity is 555.56 mg/g. The constant n of Freundlich model is 3.066, indicating that MO is very favorably adsorbed by the QBF.

3.2.5. Effect of ionic strength

It is very necessary to investigate ionic strength influence because the potential dye solution often contains some

Table 1
Parameters of kinetic model of quaternized bamboo fiber for methyl orange

Model	Parameters	Methyl orange
Pseudo-first-order	k_1 (h⁻¹)	0.0882
	Q_e (mg/g)	80.230
	R^2	0.9950
Pseudo-second-order	k_2 (g/(mg·min))	0.0026
	Q_e (mg/g)	84.460
	R^2	0.9984
Intraparticle diffusion	K_{id1}	15.099
	I_{d1}	–0.4681
	R^2	0.9979
	K_{id2}	6.7237
	I_{d2}	33.813
	R^2	0.9514
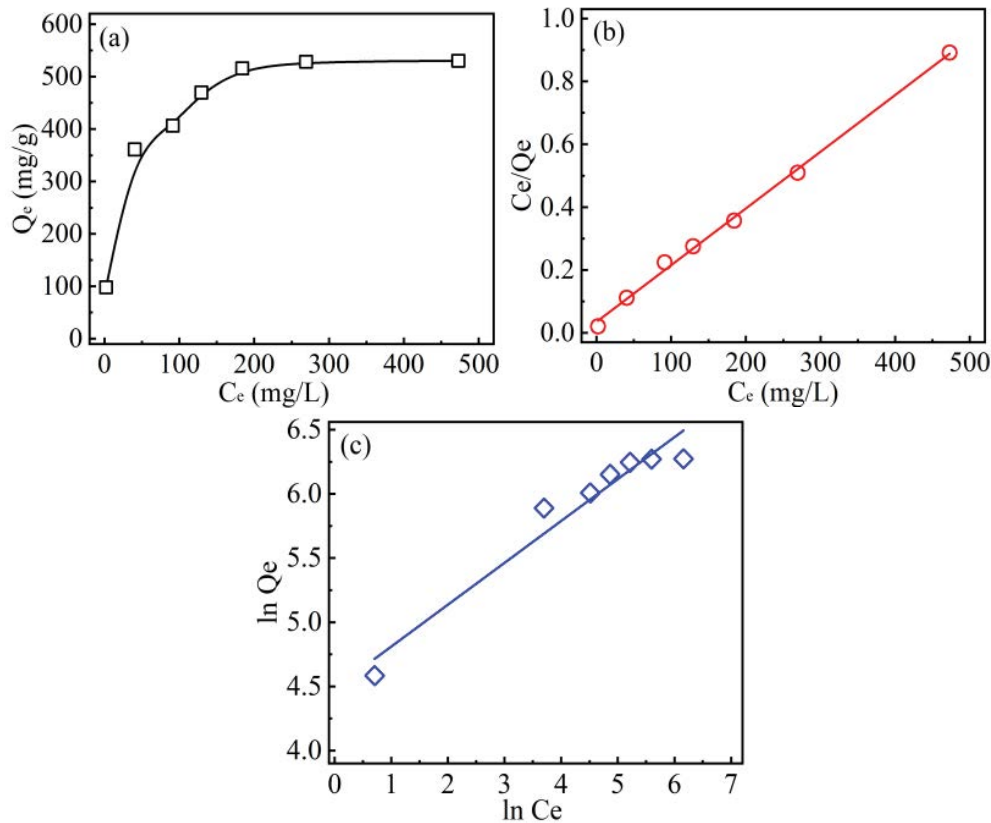
Fig. 8. Adsorption isotherms of methyl orange by quaternized bamboo fiber: correlation between the equilibrium concentration and adsorption capacity (a), Langmuir model (b), and Freundlich model (c).
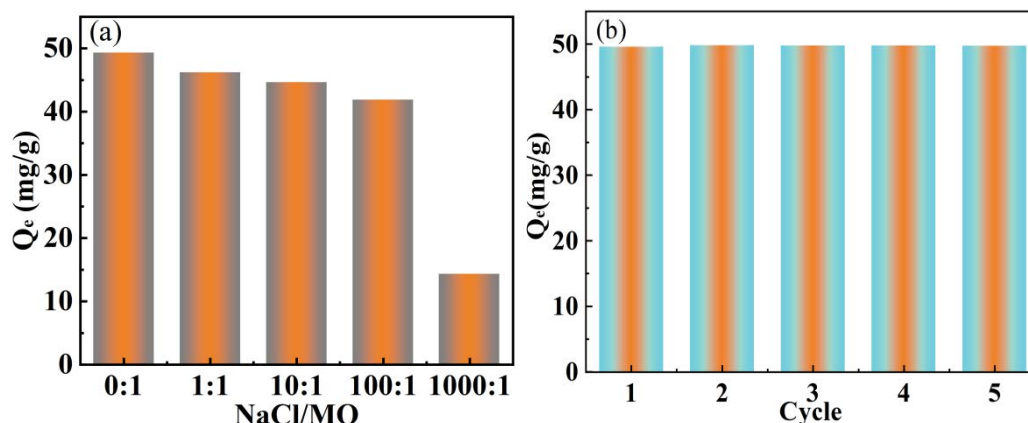
Fig. 9. Effect of NaCl on the adsorption capacity (a) and removal efficiency of methyl orange after 5 times regeneration (b).

Table 2
Langmuir and Freundlich isotherm parameters and correlation coefficient

	Langmuir			Freundlich	
Q_m (mg/g)	k_L (L/mg)	R^2	k_F (mg/g)	n	R^2
555.56	0.0515	0.9970	88.646	3.0660	0.9350

inorganic salts. The effect of NaCl on the adsorption capacity of MO is shown in Fig. 9a. The molar concentration of the MO was maintained at 0.1 mol/L and the molar concentration of NaCl is increased. The *x*-axis presents the molar ratio of NaCl/MO. With an increasing molar ratio of NaCl/MO, the adsorption capacity was decreased. When the concentration of NaCl was 1,000 times that of the MO, the adsorption capacity exhibited a decreasing trend. The results show that the primary adsorption mechanism was electrostatic adsorption and ion exchange.

3.2.6. Regeneration and reusability

The regeneration tests were conducted and the results are shown in Fig. 9b. After fully saturated adsorption (0.05 g in 50 mL, 50 mg/L), the MO loaded QBF was desorbed using 1 M HCl. After 5 adsorption–desorption cycle tests, the adsorption capacity of MO still remained unchanged. The results suggest that QBF adsorbent can be effectively regenerated by 1 M HCl and used repeatedly for MO removal.

4. Conclusions

In this study, QBF was successfully prepared through electron radiation induced graft-polymerization. Initially, GMA was grafted onto BF. Then DEAPA was successfully grafted onto the surface of BF through a ring opening reaction between the amine of 3-diethylaminopropylamine and the epoxy group of GMA. The results of MO adsorption by QBF showed that QBF can effectively remove MO at a wide pH range above 4. The adsorption kinetic followed a pseudo-second-order model, suggesting the adsorption was a chemical adsorption process. The adsorption isotherm was well fitted by Langmuir model, with a maximum theoretical adsorption capacity of 555.56 mg/g. The adsorption–desorption process showed that MO could be effectively desorbed by 1 M HCl. Furthermore, the adsorption capacity of QBF for MO remained unaffected over five adsorption–desorption cycles, indicating its excellent recycling capability. Therefore, the QBF prepared by radiation technique can be potentially applied to the treatment of MO dye in wastewater.

References

[1] J. Zheng, L. Du, P. Gao, K. Chen, L. Ma, Y. Liu, S. You, Mino-modified biomass for highly efficient removal of anionic dyes from aqueous solutions, J. Taiwan Inst. Chem. Eng., 119 (2021) 136–145.
[2] C. Zhang, H. Chen, G. Xue, Y. Liu, S. Chen, C. Jia, A critical review of the aniline transformation fate in azo dye wastewater treatment, J. Cleaner Prod., 321 (2021) 128971, doi: 10.1016/j.jclepro.2021.128971.
[3] S. Mahmood, A. Khalid, M. Arshad, T. Mahmood, D.E. Crowley, Detoxification of azo dyes by bacterial oxidoreductase enzymes, Crit. Rev. Biotechnol., 36 (2016) 639–651.
[4] K. Jankowska, Z. Su, J. Zdarta, T. Jesionowski, M. Pinelo, Synergistic action of laccase treatment and membrane filtration during removal of azo dyes in an enzymatic membrane reactor upgraded with electrospun fibers, J. Hazard. Mater., 435 (2022) 129071, doi: 10.1016/j.jhazmat.2022.129071.
[5] J. Wang, J. Yao, L. Wang, Q. Xue, Z. Hu, B. Pan, Multivariate optimization of the pulse electrochemical oxidation for treating recalcitrant dye wastewater, Sep. Purif. Technol., 230 (2019) 115851, doi: 10.1016/j.seppur.2019.115851.
[6] X. Liu, Z. Chen, W. Du, P. Liu, L. Zhang, F. Shi, Treatment of wastewater containing methyl orange dye by fluidized three-dimensional electrochemical oxidation process integrated with chemical oxidation and adsorption, J. Environ. Manage., 311 (2022) 114775, doi: 10.1016/j.jenvman.2022.114775.
[7] J. Liu, A. Liu, W. Wang, R. Li, W. Zhang, Feasibility of nanoscale zero-valent iron (nZVI) for enhanced biological treatment of organic dyes, Chemosphere, 237 (2019) 124470, doi: 10.1016/j.chemosphere.2019.124470.
[8] Z. Huang, T. Wang, M. Shen, Z. Huang, Y. Chong, L. Cui, Coagulation treatment of swine wastewater by the method

of *in-situ* forming layered double hydroxides and sludge recycling for preparation of biochar composite catalyst, Chem. Eng. J., 369 (2019) 784–792.

[9] Y. Wang, Y. Gao, L. Chen, H. Zhang, Goethite as an efficient heterogeneous Fenton catalyst for the degradation of methyl orange, Catal. Today, 252 (2015) 107–112.

[10] M. Visa, R.A. Carcel, L. Andronic, A. Duta, Advanced treatment of wastewater with methyl orange and heavy metals on TiO_2, fly ash and their mixtures, Catal. Today, 144 (2009) 137–142.

[11] M.A.M. Salleh, D.K. Mahmoud, A.W.A.K. Wan, A. Idris, Cationic and anionic dye adsorption by agricultural solid wastes: a comprehensive review, Desalination, 280 (2011) 1–13.

[12] J. Du, Y. Wu, D. Dong, M. Zhang, X. Yang, H. Xiong, L. Zhao, Single and competitive adsorption between Indigo Carmine and Methyl orange dyes on quaternized kapok fiber adsorbent prepared by radiation technique, Sep. Purif. Technol., 292 (2022) 121103, doi: 10.1016/j.seppur.2022.121103.

[13] Z. Dong, J. Du, A. Wang, X. Yang, L. Zhao, Removal of methyl orange and acid fuschin from aqueous solution by guanidinium functionalized cellulose prepared by radiation grafting, Radiat. Phys. Chem., 198 (2022) 110290, doi: 10.1016/j.radphyschem.2022.110290.

[14] M.T. Yagub, T.K. Sen, S. Afroze, H.M. Ang, Dye and its removal from aqueous solution by adsorption: a review, Adv. Colloid Interface Sci., 209 (2014) 172–184.

[15] M.S. Gohr, A.I. Abd-Elhamid, A.A. EI-Shanshory, H.M.A. Soliman, Adsorption of cationic dyes onto chemically modified activated carbon: kinetics and thermodynamic study, J. Mol. Liq., 346 (2022) 118227, doi: 10.1016/j.molliq.2021.118227.

[16] W. Li, B. Mu, Y. Yang, Feasibility of industrial-scale treatment of dye wastewater via bio-adsorption technology, Bioresour. Technol., 277 (2019) 157–170.

[17] S. Adithya, P. Muthamilselvi, K. Ashish, P. Sivaraman, Valorization of food waste as adsorbents for toxic dye removal from contaminated waters: a review, J. Hazard. Mater., 424 (2022) 127432, doi: 10.1016/j.jhazmat.2021.127432.

[18] W.B. Mbarek, L. Escoda, J. Saurina, E. Pineda, F.M. Alminderej, M. Khitouni, J.J. Sunol, Nanomaterials as a sustainable choice for treating wastewater: a review, Materials, 15 (2022) 8576, doi: 10.3390/ma15238576.

[19] S. Dutta, B. Gupta, S.K. Srivastava, A.K. Gupta, Recent advances on the removal of dyes from wastewater using various adsorbents: a critical review, Mater. Adv., 2 (2021) 4497–4531.

[20] S. Khandaker, M.T. Hossain, P.K. Saha, U. Rayhan, A. Islam, T.R. Choudhury, M.R. Awual, Functionalized layered double hydroxides composite bio-adsorbent for efficient copper(II) ion encapsulation from wastewater, J. Environ. Manage., 300 (2021) 113782, doi: 10.1016/j.jenvman.2021.113782.

[21] L. Wang, Application of activated carbon derived from "waste" bamboo culms for the adsorption of azo disperse dye: kinetic, equilibrium and thermodynamic studies, J. Environ. Manage., 102 (2012) 79–87.

[22] Q. Zhang, Y. Zeng, X. Xiao, P. Deng, Q. He, T. Zhang, Investigation on the preparation and adsorption performance of bamboo fiber based activated carbon, Fibers Polym., 20 (2019) 293–301.

[23] Y. Jiao, C. Wan, J. Li, Synthesis of carbon fiber aerogel from natural bamboo fiber and its application as a green high-efficiency and recyclable adsorbent, Mater. Des., 107 (2016) 26–32.

[24] Y. Chen, W. Jiang, X. Luo, Y. Huang, B. Jin, H. Gao, W. Li, Z. Liang, The study of kinetics of CO_2 absorption into 3-dimethylaminopropylamine and 3-diethylaminopropylamine aqueous solution, Int. J. Greenhouse Gas Control, 75 (2018) 214–223.

[25] L. Cheng, J. Wu, H. Liang, Q. Yuan, Preparation of poly(glycidyl methacrylate) (PGMA) and amine modified PGMA adsorbents for purification of glucosinolates from cruciferous plants, Molecules, 25 (2020) 3286, doi: 10.3390/molecules25143286.

[26] A.A. Galhoum, E.A. Elshehy, D.A. Tolan, Synthesis of polyaminophosphonic acid-functionalized poly(glycidyl

[27] methacrylate) for the efficient sorption of La(III) and Y(III), Chem. Eng. J., 375 (2019) 121932, doi: 10.1016/j.cej.2019.121932.

[27] B.F. Senkal, F. Bildik, E. Yavuz, A. Sarac, Preparation of poly(glycidyl methacrylate) grafted sulfonamide based polystyrene resin with tertiary amine for the removal of dye from water, React. Funct. Polym., 67 (2007) 1471–1477.

[28] J. Du, Q. Ye, Z. Dong, X. Yang, L. Zhao, Selective adsorption of mercury(II) ions from aqueous solution by two kinds of modified cellulose microsphere, Desal. Water Treat., 229 (2021) 302–313.

[29] X. Yang, Q. Pan, Y. Ao, J. Du, L. Zhao, Facile preparation of L-cysteine modified cellulose microspheres as a low-cost adsorbent for selective and efficient adsorption of Au(III) from the aqueous solution, Environ. Sci. Pollut. Res., 27 (2020) 38334–38343.

[30] J. Du, Z. Dong, X. Yang, L. Zhao, Radiation grafting of dimethylaminoethyl methacrylate on cotton linter and subsequent quaternization as new eco-friendly adsorbent for phosphate removal, Environ. Sci. Pollut. Res., 27 (2020) 24558–24567.

[31] Z. Dong, J. Du, Y. Chen, M. Zhang, L. Zhao, A comparative study of immobilizing ammonium molybdophosphate onto cellulose microsphere by radiation post-grafting and hybrid grafting for cesium removal, Environ. Pollut., 273 (2021) 116432, doi: 10.1016/j.envpol.2021.116432.

[32] J. Du, Z. Dong, D. Wen, X. Yang, M. Zhai, R. Hua, L. Zhao, Selective recovery of rhenium from the simulating leaching solutions of uranium ore by amino guanidine functionalized microcrystalline cellulose microsphere, J. Mol. Liq., 360 (2022) 119399, doi: 10.1016/j.molliq.2022.119399.

[33] J. Du, M. Zhang, Z. Dong, X. Yang, L. Zhao, Facile fabrication of tannic acid functionalized microcrystalline cellulose for selective recovery of Ga(III) and In(III) from potential leaching solution, Sep. Purif. Technol., 286 (2022) 120442, doi: 10.1016/j.seppur.2022.120442.

[34] J. Du, D. Fan, Z. Dong, X. Yang, L. Zhao, Fabrication of quaternized sisal fiber by electron beam radiation and its adsorption of indigo carmine from aqueous solution, Cellulose, 29 (2022) 5137–5149.

[35] Z. Dong, Y. Wang, D. Wen, J. Peng, L. Zhao, M. Zhai, Recent progress in environmental applications of functional adsorbent prepared by radiation techniques: a review, J. Hazard. Mater., 424 (2021) 126887, doi: 10.1016/j.jhazmat.2021.126887.

[36] X.H. Pan, J.H. Zu, A highly hydrophilic cation exchange nonwoven with a further modifiable epoxy group prepared by radiation-induced graft polymerization, Polym. Chem., 12 (2021) 5796–5802.

[37] M. Zhang, J. Chen, M. Wang, R. Li, G. Wu, Electron beam-induced preparation of AIE non-woven fabric with excellent fluorescence durability, Appl. Surf. Sci., 541 (2020) 148382, doi: 10.1016/j.apsusc.2020.148382.

[38] J. Du, H. Xiong, Z. Dong, X. Yang, L. Zhao, J. Yang, Ethylenediamine and pentaethylene hexamine modified bamboo sawdust by radiation grafting and their adsorption behavior for phosphate, Appl. Sci., 11 (2021) 7854, doi: 10.3390/app11177854.

[39] J. Du, Y. Wu, Z. Dong, M. Zhang, X. Yang, H. Xiong, L. Zhao, Single and competitive adsorption between Indigo Carmine and Methyl orange dyes on quaternized kapok fiber adsorbent prepared by radiation technique, Sep. Purif. Technol., 292 (2022) 121103, doi: 10.1016/j.seppur.2022.121103.

[40] D. Chattopadhyay, K. Umrigar, Chemical modification of waste cotton linters for oil spill cleanup application, J. Inst. Eng. India Ser. E, 98 (2017) 103–120.

[41] X. Yu, S. Tong, M. Ge, L. Wu, W. Song, Synthesis and characterization of multi-amino-functionalized cellulose for arsenic adsorption, Carbohydr. Polym., 92 (2013) 380–387.

[42] X. Lv, Y. Li, M. Yang, Humidity sensitive properties of copolymer of quaternary ammonium salt with polyether-salt complex, Polym. Adv. Technol., 20 (2009) 509–513.

[43] S. Deng, Y. Zheng, F. Xu, B. Wang, J. Huang, G. Yu, Highly efficient sorption of perfluorooctane sulfonate and perfluorooctanoate

on a quaternized cotton prepared by atom transfer radical polymerization, Chem. Eng. J., 193 (2012) 154–160.

[44] H.S. Elbogami, R.G. El-Sharkawy, B.A.A. Balboul, Adsorption of Direct red 81 dye onto friendly prepared iron oxide/ multi-walled carbon nanotubes nanocomposite: kinetics and thermodynamic studies, Desal. Water Treat., 294 (2023) 247–258.

[45] J. Li, Adsorption of Cd(II) and Pb(II) by Mg-modified straw biochar, Desal. Water Treat., 292 (2023) 131–140.

[46] J. Du, X. Yang, H. Xiong, Z. Dong, Z. Wang, Z. Chen, L. Zhao, Ultrahigh adsorption capacity of acrylic acid-grafted xanthan gum hydrogels for Rhodamine B from aqueous solution, J. Chem. Eng. Data, 66 (2021) 1264–1272.